Enhancement of the Critical Heat Flux by Using Heat Spreader

Yong-Sik Yoon
Korea Aerospace Institute, Taejon, 305-600, Korea
Hyup Yang
Samchok National University, Samchok, 245-711, Korea
Ho-Young Kwak*
Department of Mechanical Engineering, Chung-Ang University, 221, Huksuk-dong, Dongjak-gu, Seoul 156-756, Korea

Direct immersion cooling has been considered as one of the promising methods to cool high power density chips. A fluorocarbon liquid such as FC-72, which is chemically and electrically compatible with microelectronic components, is known to be a proper coolant for direct immersion cooling. However, boiling in this dielectric fluid is characterized by its small value of the critical heat flux. In this experimental study, we tried to enhance the critical heat flux by increasing the nucleate boiling area in the heat spreader (Conductive Immersion Cooling Module). Heat flux of 2 MW/m^2 was successfully removed at the heat source temperature below 78℃ in FC-72. Some modified boiling curves at high heat flux were obtained from these modules. Also, the concept of conduction path length is very important in enhancing the critical heat flux by increasing the heat spreader surface area where nucleate boiling occurs.

Key Words : CHF, Conduction Path Length, Heat Spreader, Immersion Cooling, Microelectronics Cooling

Nomenclature

A_{chip}: Chip surface area
I : Current to the heater (chip)
q'' : Heat flux of chip
q_{chip} : Heat dissipation rate in chip
T_s : Saturated temperature of liquid
T_w : Temperature of chip
V : Voltage across the heater (chip)

Greek Letters

ΔT_s : Wall superheat $(=T_w-T_s)$

1. Introduction

Continuing efforts to achieve high circuit performance in electronic packages have resulted in high power density at both chip and module levels. The power dissipation density at these levels has already exceeded the air cooling capacity of the packages and is expected to exceed 1~2 MW/m^2, which can only be cooled by a new technique. Therefore, thermal management of electronic package is important in maintaining or improving reliable package operation since the temperature of all components must be kept within their specified limit (Chu and Simon, 1984).

Direct immersion cooling (Simon, 1987) has been considered as one of the promising methods to cool such high power density chips. A fluorocarbon liquid such as FC-72 is a prime candidate for direct immersion cooling since it is chemically and electrically (high dielectric strength) compatible with microelectronic components (Mudawar and Maddox. 1990). Furthermore, this liquid has a boiling point of 56℃ at atmospheric pressure ; hence, it is capable of maintaining the

* Corresponding Author,
E-mail : kwakhy@cau.ac.kr
TEL : +82-2-820-5278; **FAX** : +82-2-826-7464
Department of Mechanical Engineering, Chung-Ang University, 221, Huksuk-dong, Dongjak-gu, Seoul 156-756, Korea. (Manuscript **Received** April 24, 2002; **Revised** April 14, 2003)

Table 1 Selected thermal properties of a Fluorinert FC-72

Normal boiling point at 1 atm	56℃
Liquid density at 25℃	1680 kg/m^3
Vapor density at boiling point	14 kg/m^3
Specific heat at 25℃	1.045 kJ/kg
Heat of vaporization at boiling point	87.78 kJ/kg
Thermal conductivity at 25℃	0.057 W/mK
Surface tension at 25℃	0.012 N/m
Average molecular weight	340

temperature of the chip surface below 85℃ against chip failure (Simon, 1983) when pool or forced convection boiling is employed for immersion cooling of the chip. However, this liquid possesses poor thermal transfer properties compared to the common fluids such as water. This dielectric liquid, especially, shows high wetting behavior that causes it to have unusually high incipient boiling superheat (You et al. 1991). As a result of this, boiling in dielectric fluids is characterized by its relatively small value of the critical heat flux (CHF) about 0.2 MW/m^2 (Marto and Lepere, 1982). Thus, further CHF enhancement is essential for meeting the present R&D target of cooling (Bar-Cohen et al., 1989). Some selected thermal properties for FC-72 are listed in Table 1.

Many have been tried to enhance CHF or the maximum cooling limit. Nakayama et al. (1984) achieved the heat flux level of above 1 MW/m^2 with $\triangle T_s = T_w - T_s$ (wall superheat) $\cong$40℃ in FC-72 by attaching studs covered with miniature fins to the surface of heat source. Gu et al. (1984) obtained CHF of 1.41 MW/m^2 at the value of $\triangle T_s$=70℃ in a curved channel with subcooling of 38℃ and flow velocity of 4 m/s in FC-72. Also Mudawar and Maddox (1990) achieved CHF as high as 3.61 MW/m^2 with $\triangle T_s$=55℃ by combining subcooling of 48℃, flow velocity of 4.1 m/s, and surface modification with pin fins in FC-72. Using a square-shaped stud in a diamond configuration, Anderson and Mudawar (1989) obtained a CHF as high as 0.63 MW/m^2 in FC-72. Recently, a microporous coating that increases the nucleate boiling heat transfer coefficient by 300% and the critical heat flux by 500% has been developed (Chang and You, 1997). Very recently, the critical heat flux enhancement resulting from stream wise curvature was tested by Sturgis and Mudawar (1999). Several studies have also been done to reduce the incipient boiling superheat by using porous metallic coatings (Bergles and Chyu, 1982), by using augmented silicon surfaces (Bhavnani et al., 1993), and by using pored structural surface (Nakayama et al., 1982).

In this experimental study, we tried to enhance CHF by increasing the nucleate boiling area in the heat spreader surface by conduction heat transfer, a method which has never been investigated. The immersion cooling method by using the heat spreader is named as the "Conductive Immersion Cooling Module (CICM)" and its mechanism is as follows. This module simply applies the immersion cooling method by using a chip-spreader device (Kadambi and Abuaf, 1983). Applying power to the chip above some limit, the heat transfer from the chip is conducted into the upper and side surfaces of the heat spreader, boiling both surfaces. One of the distinct features in this experiment is that the heater was fabricated from n-type silicon wafer.

The heat conduction through the bottom surface of the chip to the heat spreader enabled the modules to increase the nucleate boiling area in the heat spreader at very high heat flux. The increase in the boiling area successfully removed the heat flux as much as 2 MW/m^2 while chip surface temperature was maintained below 78℃ ($\triangle T_s$=22℃) in FC-72. The amount of heat removed by the module without subcooling and convective effect was about 10 times higher than the CHF obtained in FC-72. Therefore, this module is very suitable for cooling high powered microelectronic devices by pool boiling. In addition, these modules provided modified boiling curves at high fluxes.

2. Experimental Apparatus and Procedures

2.1 Experimental apparatus

A typical pool boiling vessel utilized in this experiment is shown in Fig. 1. The main com-

ponents of the test facility used are a boiling vessel, a charging tank, and measurement and control system. The boiling vessel with dimension of 160 mm × 160 mm × 500 mm was made of aluminum. Quartz sight glass windows to facilitate visual observation were made on the front and real walls of the vessel with brass flanges. The top cover of the vessel made of brass has taps for thermocouple connectors, manometer, power cable, liquid supply line, and vapor line to the charging tank. The charging tank with argon gas supplied the working fluid. A Fluorinert FC-72 used as working fluid was heated by external teflon coated nichrome wire heater wrapped around the vessel. Heat was removed from the vessel via a water cooled condenser coiled within the upper section of the vessel. The bulk fluid temperature was measured by a K-type thermocouple located near the test module. A temperature controller (OMEGA, Module, E924K29) powered the external nichrome heater to maintain the liquid temperature. The pressure of the vessel was maintained by controlling the water stream through the condenser.

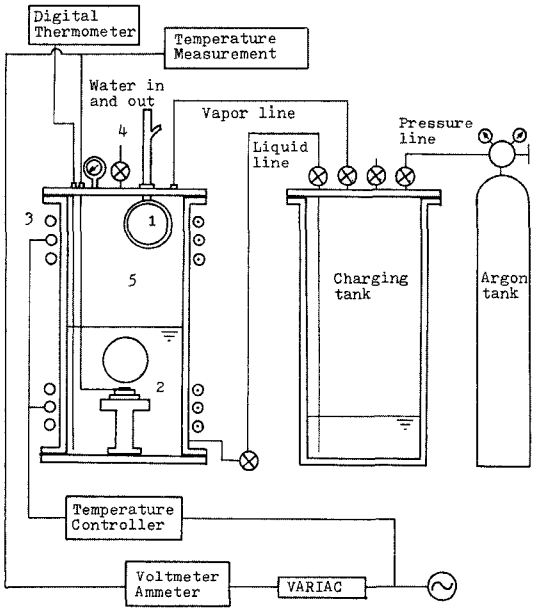

Fig. 1 Schematic of test facility for boiling on chip : 1) condenser, 2) chip, 3) wire heater, 4) pressure relief valve, 5) test chamber

2.2 Conductive immersion cooling module (CICM)

The CICMs are schematically shown in Fig. 2. Two types of the module were fabricated and tested. One is that chip (silicon wafer ; thermal conductivity at 300 K is 156 W/mK) with thickness of 0.8 mm was mounted on the upper surface of heat spreader made of copper (thermal conductivity ; 401 W/mK) as shown in Fig. 2(a). This is a typical structure of a power IC (Cstello and Antognetti, 1978). The other is that the chip was embedded in the upper surface of heat spreader (Fig. 2(b)) which was mounted on the top of relatively large epoxy glass plate.

A layer of RTV silicon elastomer (Shin Etsu Co., KE3493 with thermal conductivity of 1.6 W/mK) having approximately 1 mm thickness was inserted between the chip and heat spreader for solid attachment and electrical insulation. The temperatures of the chip and heat spreader were measured by calibrated T-type thermocouples located at the centers of the upper and bottom surfaces of heat spreader. All T type thermocouples used were calibrated with a DC voltage/current standard generator (Yokokawa, 2553) so that the accuracy of the measured temperature is about ±0.1℃. The junction of the upper thermocouple was carefully made to come in contact with the chip.

A 0.17 mm diameter copper wire welded to the

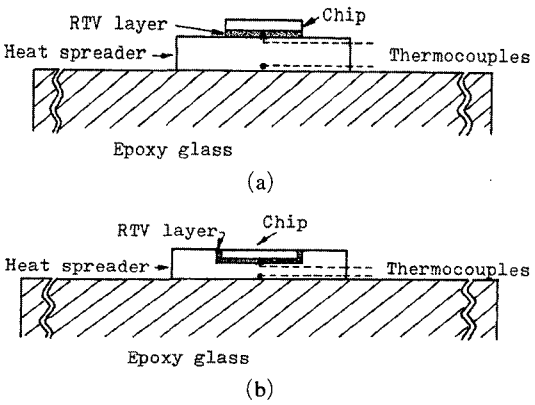

Fig. 2 Conductive immersion cooling modules. (a) the chip is mounted on the heat spreader and (b) the chip is embedded in the heat spreader

Table 2 Chip and heat spreader dimensions, heat transfer area, and the characteristic length for heat conduction of the modules tested

Module name	Chip dimension (mm)	Heat spreader dimension (mm)	Heat transfer area, As (mm^2)	Characteristic length for heat conduction (mm)
ASA1	5×5	7.5×7.5×4	151	1.49
ASA3	5×5	10×10×3	195	1.54
ASA4	5×5	10×10×4	235	1.70
ASA5	5×5	10×20×4	415	1.93
ASA6	5×5	10×10×6	315	1.90
BSB4	5×10	10×20×4	390	2.05
BSB6	5×10	10×20×6	510	2.35

n-type silicon wafer by using indium was used as a power cable. The power input to the chip was calculated by measuring the voltage across the chip and the input current to the chip. In this calculation, the power dissipation in the very thin wire of the power cable was taken into account. The resistance of the chip varied slightly depending on the chip temperature.

The CICMs tested are classified by the sizes of the chip and spreader as shown in Table 1. The characteristic lengths for heat conduction of the modules were calculated by dividing the volume by the heat transfer area of the heat spreader. The modules with chip embedded in the heat spreader are named by adding a letter N to the end of the module name listed in Table 2.

2.3 Experimental procedures

The boiling vessel was cleaned with acetone before each module test. Leak test for the boiling vessel and the charging tank was done by charging argon gas to the vessels and leaving the system alone without supply of the gas. The pressure of the system remained the same for two hour or so until the system pressure reached 3 atm. The liquid level was maintained at about 10 cm above the top of the module. The external nichrome heater was energized to raise the fluid temperature to the desired saturated condition. At the start of run, the pool was boiled to saturated condition and the power to the heater was turned on at 60 kW/m^2 and the pressure relief valve was opened for a minute to degas the test liquid. The pressure in the test chamber was monitored by a pressure gauge attached to the chamber. This process was enough to eliminate the dissolved gas effect on nucleate boiling. In fact, air concentration in FC-72 at 25℃ is as much as 4.0×10^{-3}, which might affect the cessation of boiling (You et al., 1990). However, at the saturation condition at 1 atm, the air concentration reduces to 2.0×10^{-4}, at which the dissolved air does not affect either incipience or cessation of boiling.

When the system was stabilized to saturated condition, the power to the test module was started at 1 V and increased by 1 V up to the maximum attainable heat flux. For some cases, the power was then decreased in the same way voltage was increased to observe the boiling hysteresis. At each power level, the system was allowed to reach steady state for 10 minutes, and following data were obtained: (1) the voltage drop across the chip, (2) current to the chip, (3) vapor and liquid temperatures of the working fluid, and (4) the temperatures of the chip and heat spreader.

The heat flux was calculated by using the following equation by assuming that uniform heat generates within the silicon wafer;

$$q''=q_{chip}/A_{chip} \tag{1}$$

q_{chip} in Eq. (1) is equal to the voltage×the current to the chip. The voltage to the chip was measured by a digital voltmeter, which is accurate within the range of 0.01 V. The current to the chip was determined by measuring the voltage drop across a resistor connected with a series of chips. The accuracy of the current measured is

less than ±0.05 A so the estimated uncertainty in the heat flux is about ±11% at low powers and ±7% at high powers with accounting for the error in the measurement of the chip surface area of ±4%. The relative errors of the heat flux may be estimated by using the following equation.

$$\frac{|\Delta q''|}{q''}=\pm\left(\frac{|\Delta q_{chip}|}{q_{chip}}+\frac{|\Delta A_{chip}|}{A_{chip}}\right)$$
$$=\pm\left(\frac{\Delta I}{I}+\frac{|\Delta V|}{V}+\frac{|\Delta A_{chip}|}{A_{chip}}\right) \quad (2)$$

3. Experimental Results and Discussions

It is well known that the maximum cooling limit achieved by immersion cooling can not exceed the CHF. At this limit, the temperature of the boiling surface may increase abruptly when slightly-increased heat flux is applied. Consequently, any boiling system should be operated below this limit. In this study, we focused on the enhancement of the cooling limit by using the CICM.

Figure 3(a) is the boiling curve obtained by from the standard module, ASA4; that is from a 5 mm×5 mm chip mounted on the heat spreader of 10 mm×10 mm×4 mm. In Fig. 3(b), the boiling curves were obtained from the vertical channel with gap of 26 mm (Jeon et al, 2001) along with the data obtained from a plain tube by Marto and Lepere (1982) and a microporous surface by Chang and You (1997) for comparison purpose. For FC-72, the CHF was found to be 0.2 MW/m^2 at the wall superheat of 30℃ for a plain tube and at the superheat of 10~20℃ for

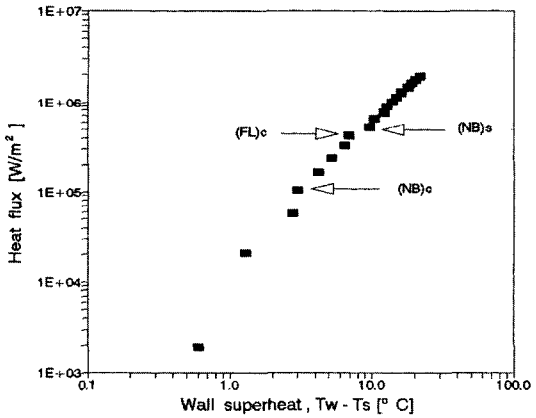

(a)

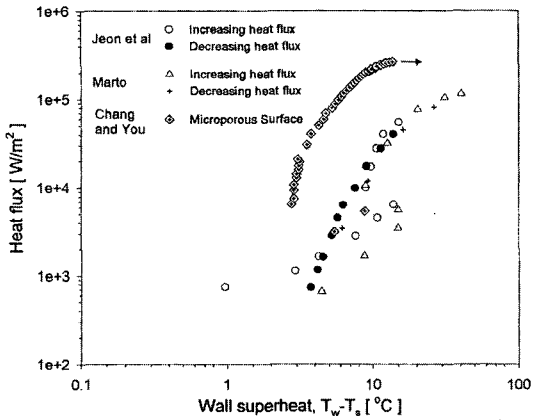

(b)

Fig. 3 (1) Pool boiling curve for the ASA4 module, and (2) pool boiling curves obtained from plain and microporous surfaces

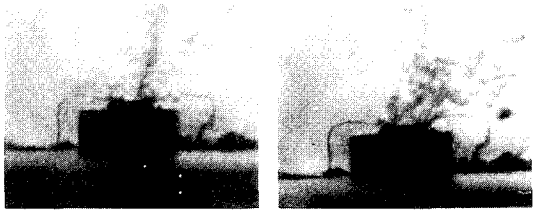

(a) 57.3 kW/m^2 (b) 165.7 kW/m^2

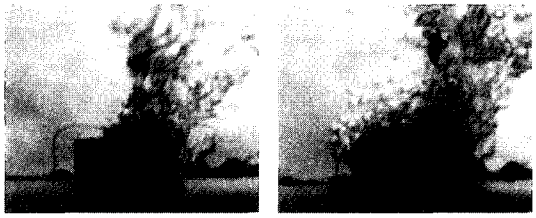

(c) 636.1 kW/m^2 (d) 876.7 kW/m^2

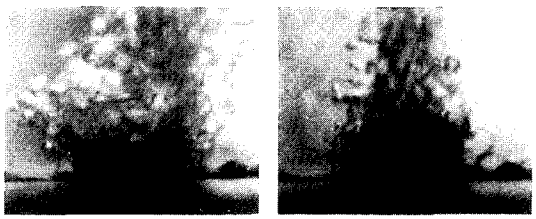

(e) 1.29 MW/m^2 (f) 1.60 MW/m^2

Fig. 4 Photographs of boiling on the surface of the ASA4 Module. The numbers in the photographs indicate the heat fluxes applied

enhanced surface (Marto and Lepere, 1982), as shown in Fig. 3(b). However, a higher CHF in FC-72 was achieved by using a microporous surface. Also the selected photographs in Fig. 4 show the boiling on the surface of the module. An explanation for the boiling curve which shows the details about the boiling on the ASA4 module, and selected photographs are as follows.

The temperature overshoot and boiling curve hysteresis, which usually occur for plain surface (Marto and Lepere, 1982 ; Jeon et al., 2001), can not be seen in the boiling curve obtained from ASA4 module. These phenomena may occur because of patch boiling developed on the welding point at modest heat flux of 57.3 kW/m^2 (Fig. 4(a)). As heat flux is increased to 165.7 kW/m^2, vigorous boiling occurs on the whole region of the chip (Fig. 4(b)). Nucleate boiling on the chip persists until DNB (Departure of Nucleate Boiling) on the heater surface of the chip occurs. At this stage, a small increase in heat flux may increase the surface temperature, and the heat transfer through the upper surface of the chip reaches its maximum limit, which can be considered as CHF, or film boiling limit denoted as $(FL)_C$ occurs on the chip at 428.3 kW/m^2 as shown in Fig. 3(a). The temperature difference between the chip and heat spreader is less than 1.5℃ up to this point, as can be found from Table 3. Additional heat, which cannot escape through the upper surface of the chip at this point because the maximum heat transfer does exceed CHF, is conducted to the heat spreader so that nucleate boiling on the upper and side surfaces of the heat spreader (Fig. 4(c)) occurs. This is why the temperature increase at the DNB in the boiling curve is fairly small. In other words, the boiling on the surface of the heat spreader prevents the abrupt increase of the chip's temperature. This phenomenon is described as nucleate boiling for spreader, denoted as $(NB)_S$ at the heat flux of 524.9 kW/m^2 as shown in Fig. 3(a). When the

Table 3 The temperatures of chip and heat spreader and observed boiling phenomena for different heat fluxes applied to the ASA4 module

Heat flux (kW/m^2)	Heat spreader temp.(℃)	Chip temp.(℃)	Observed phenomena
20.9	57.3	56.9	Boiling at welding point
57.3	58.8	57.6	Fig. 4(a)
105.0	59.0	58.0	Nucleate boiling starts on chip
165.7	60.2	59.0	Vigorous nucleate boiling on chip ; Fig. 4(b)
240.2	61.2	59.5	
328.4	62.5	60.0	
428.3	62.9	60.5	Film boiling on chip
524.9	65.6	61.0	Nucleate boiling on the surface of heat spreader
636.1	66.5	61.5	Vigorous nucleate boiling on the RHS of heat spreader ; Fig.4(c)
753.3	68.2	62.0	
876.7	68.8	62.5	Vigorous nucleate boiling on the heat spreader ; Fig.4(d)
1002.0	70.0	63.0	
1146.0	71.0	63.5	
1286.0	72.1	64.0	Fig. 4(e)
1460.0	74.0	64.5	
1596.0	75.1	65.0	Fig. 4(f)
1752.0	76.5	65.5	
1910.0	77.8	65.9	

power applied to the chip is increased, nucleate boiling on the upper surface of heat spreader occurs vigorously (Fig. 4(d)). After this stage, the wall superheat of the chip and the temperature difference between the chip and the heat spreader increase steadily as the power increases. Nucleate boiling occurs on the heat spreader at the wall superheat of 10.5℃ (Fig. 4(f)). The maximum heat flux obtained by this module, ASA4, is about 2 MW/m^2 at the wall superheat, 22℃. The maximum heat flux occurs because the increase in the surface area of nucleate boiling on the heat spreader is 3~4 times than that of the nucleate boiling area at $(NB)_S$. Such high heat flux cannot be achieved by attaching four pin fins above the boiling surface (Mudawar and Maddox, 1990), which provide the maximum heat flux of about 1.8 MW/m^2 even with subcooling of 6.0℃ and moderate flow velocity of 2.25 m/s. Such moderate increase in CHF is because the modified surface suggested by Mudawar and Maddox (1990) was successful in increasing the heat transfer area substantially but failed in increasing the boiling area very much. At the maximum heat flux, the temperature at the upper side of heat spreader is about 65.6℃. After this point, typical film boiling behavior over the chip and heat spreader prevails. Table 2 gives the temperatures of silicon wafer and heat spreader and the observed boiling phenomena as a function of the heat flux applied to the ASA4 module.

Figure 5 is the boiling curve for the BSB4 module. Much the same interpretation as for ASA4 can be applied to this boiling curve even though the sudden increase in the temperature at the DNB is larger than that observed on ASA4. With this module, the maximum heat flux applied at the wall superheat of 23℃ is 1 MW/m^2, which is one half of the maximum heat flux achieved on ASA4 module. However, for ASA4N module, where the chip was embedded in the heat spreader, the boiling curve shown in Fig. 6 is dramatically different from that for ASA4. At the heat flux of 463 kW/m^2, the chip temperature rose rapidly from 68℃ to 100℃. This increase is typical at the CHF, as shown in Fig. 3(b). At this limit, the temperature of the chip fluctuated very

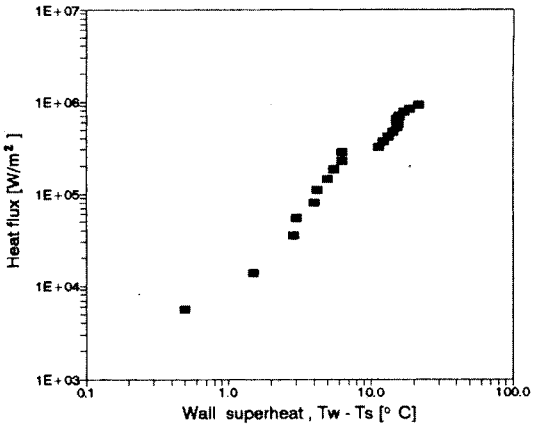

Fig. 5 Pool boiling curve for the BSB4 module

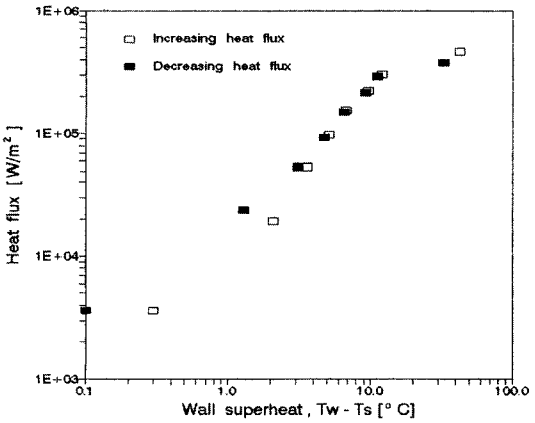

Fig. 6 Pool boiling curve for the ASA4N module

rapidly, and this fluctuation made it difficult to measure the quantity. The maximum heat flux of 0.27 MW/m^2 at the wall superheat of 26℃ for ASA4N module is almost same as that obtained from the surface of plain tube by Marto and Lepere (1982) as shown in Fig. 3(b).

Some photographs of boiling phenomena on the surfaces of the modules, BSB6 and BSB6N, are shown in Fig. 7. Surprisingly, no boiling occurred on the surface of the heat spreader for BSB6N module at heat flux of 0.20 MW/m^2. Also, a large bubble departed from the chip surface for BSB6N (Fig. 7(d)) as it is compared with the case of BAB6 (Fig. 7(b)), which means that film boiling occurs on the surfaces of chip in BSB6N module. The CHFs obtained for the modules BSB6 and BSB6N are 0.6 MW/m^2 at $\triangle T_s$=11℃

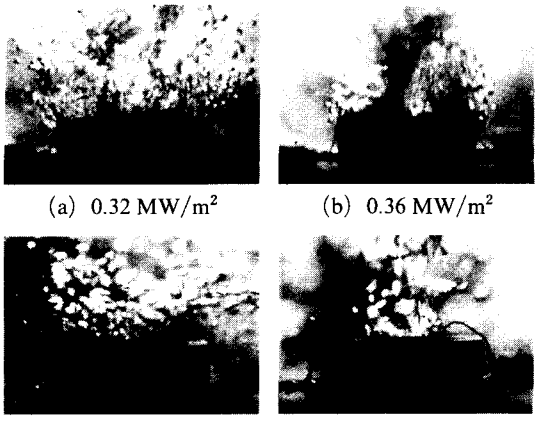

(a) 0.32 MW/m^2 (b) 0.36 MW/m^2

(c) 37.6 MW/m^2 (d) 0.20 MW/m^2

Fig. 7 Photographs of boiling on the surface of the BSB6 module (a and b) and BSB6N module (c and d). The numbers in the photographs indicate the heat fluxes applied

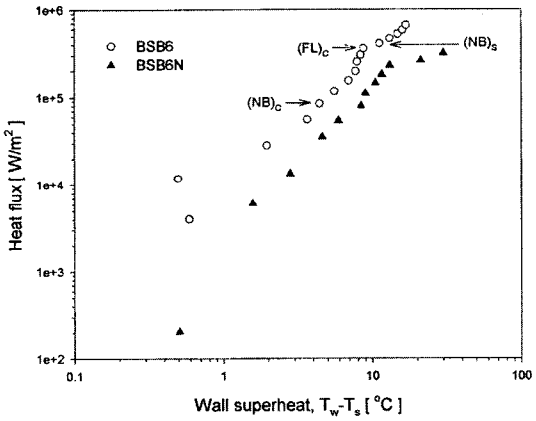

Fig. 8 Pool boiling curves for the BSB6 and BSB6N modules

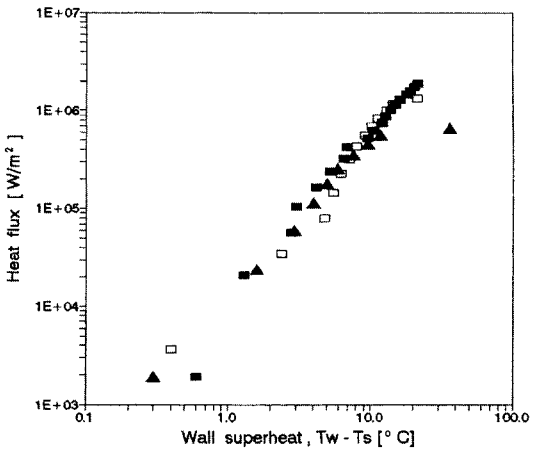

Fig. 9 Pool boiling curves for different surface areas of heat spreader. Pool boiling curves for ASA1(□), ASA4(■), and ASA5(▲) modules

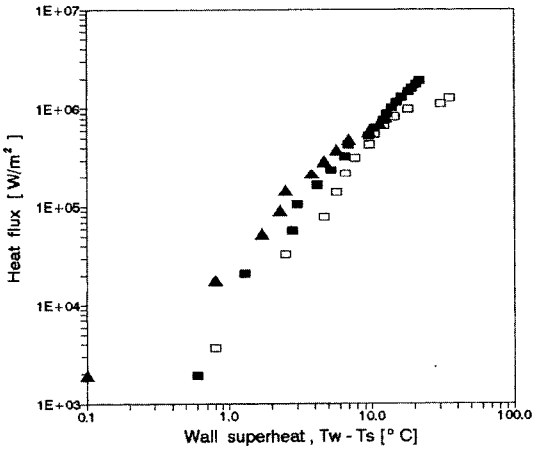

Fig. 10 Pool boiling curves for different thickness of heat spreader. Pool boiling curves for ASA3 (□), ASA4(■), and ASA6(▲) modules

and 0.2 MW/m^2 at $\triangle T_s$=12℃, respectively. The corresponding boiling curves for these modules are shown in Fig. 8. The boiling in BSB6 and BSB6N modules were the same as those in ASA4 and ASA4N modules respectively.

Various Modules were tested to get the optimum size of heat spreader. In one group of modules, the upper surface area was increased while keeping the thickness of 4 mm for heat spreader. The experimental results of this test are shown in Fig. 9, which showed that ASA4 is the best module and ASA5 is the worst module among ASA1, ASA4, and ASA5 module with respect to the CHF. This result is just due to the fact that the characteristic length scale of the ASA5 module is larger than the optimum length of 1.70 mm for ASA4 module. Next, we tested the modules, that had thickness different from that of the optimum module showing the best boiling behavior. The test results are shown in Fig. 10. Again ASA4 module was the best module among ASA3, ASA4, and ASA6.

These experimental results shown in Figs. 9 and 10 indicate that for a given chip size, the

optimum size of heat spreader exists and that a large heat spreader that has a longer conduction path has difficulties in inducing boiling on the surface of the heat spreader. As shown in Table 1, the characteristic length of heat conduction for ASA4 module, which shows the best performance in boiling heat transfer, is about 1.70 mm. However, the characteristic length of ASA5 and ASA6, which show the worst performance among the test modules, are 1.93 and 1.90, respectively. On the other hand, the module with a small heat spreader was inferior to the optimal module with respect to the boiling behavior because it has a smaller available heat transfer area than that of the optimum module. However, the conduction path length affects mostly the performance of the boiling heat transfer of the modules. This can be justified by the fact that the CHF for BSB6 module, which has the longest path length for heat conduction, is the lowest among the entire test modules.

We expected that the heat flux will spread mostly radially through the heat spreader because the thermal resistance of epoxy glass at the bottom of heat spreader is much greater than that of the heat spreader, which is legitimate because the Biot number is rather small for the heat spreader tested. In this instance, heat conduction induces boiling on the surface of the heat spreader. Heat flow along the path of least resistance in the case of small Biot number was visualized numerically by Eades et al. (1991). For the module with an imbedded chip, the heat from the chip flows mainly below the chip and dissipates inside the heat spreader, preventing boiling on the upper surface of the heat spreader. This is why this type module has same boiling behavior occurred on plain surface. Note that the amount of released heat through the substrate by conduction was also observed for a microheater imbedded in the substrate (Hijikata et al., 1997).

4. Conclusion

Various "Conductive Immersion Cooling Modules," which are simple application of immersion cooling method to chip spreader device, have been tested experimentally to increase the critical heat flux. In this method, the surface area of nucleate boiling is increased. The optimum size of the heat spreader, which removes the heat flux, as much as 2 MW/m^7 in FC-72, has been found by a series of experiments using chips of dimensions 5 mm×5 mm×0.8 mm. Such high heat flux can be removed by using a cooling module with heat spreader having a characteristic length for heat conduction of about 1.70 mm. This condition shows that the conduction path length is a crucial parameter in the induction of nucleate boiling on the heat spreader. However, this mechanism should be studied numerically in more detail.

References

Anderson, T. M., and Mudawar, I, 1989, "Microelectronic Cooling by Enhanced Pool Boiling of a Dielectric Fluorocarbon Liquid," *J. Heat Transfer*, Vol. 111, pp. 752~759.

Bar-Cohen, A., Mudawar, I. and Whalen, B., 1986, "Future Challenges for Electronic Cooling," Research Needs in Electronic Cooling, F. P. Incropera, ed., published by the National Science Foundation and Perdue University, West Lafayette, IN, pp. 70~77.

Bergles, A. E. and Chyu, M. C., 1982, "Characteristics of Nucleate Pool Boiling from Porous Metallic Coatings," *J. Heat Transfer*, Vol. 104, pp. 279~285.

Bhavnani, S. H., Tsai, C., Jaeger, R. L. and Eison, D. L., 1993, "An Integral Heat Sink for Cooling Microelectronic Components," *J. Heat Transfer*, Vol. 115, pp. 284~291.

Chang, J. Y. and You, S. M., 1997, "Enhanced Boiling Heat Transfer from Micro-Porous surfaces - Effects of a coating composition and method," *Int. J. Heat Mass Transfer*, Vol. 40, pp. 4449~4460.

Chu, R. C. and Simon, R. E., 1984, "Thermal Management of Large Scale Digital Computers," *The International Society for Hybrid Micro Electronics*, Vol. 7, pp. 35~43.

Cstello, R. and Antognetti, P., 1978, *IEEE J. of Solid-State Circuits*, Vol. SC-13, pp. 363~366.

Eades, H. H. and Nelson, D. J., 1991, "Thermal Interaction of High-Density Heat Sources on Ceramic Substrates," in *ASME/JSME Thermal Engineering Proceedings*, Vol. 2, pp. 349~356.

Gu, C. B., Chow, L. C. and Beam, J. E., 1989, "Flow Boiling in a Curved Channel," in *Heat Transfer in High Energy/High Heat flux Applications*, HTD-Vol. 119, Goldstein, R. J., et al ed., pp. 25~33.

Hijikata, K., Yamamoto, N. and Takagi, S., 1997, "Boiling Heat Transfer from a Micro Heater," in DSC-Vol. 62, HTD-Vol. 354, *Microelectromechanical Systems (MEMS)*, pp. 135~142.

Jeon, J., Na, J., Park, H. and Kwak, H., 2001, "An Experiment on Thermosyphon Boiling in Uniformly Heated Vertical Tube and Asymmetrically Heated Vertical Channel," *KSME Int. J.*, Vol. 15, pp. 98~107.

Kadambi, V. and Abuaf, N., 1983, "Axisymmetric and Three Dimensional Chip-Spreader Calculations," *Proceedings of the 1983 National Heat Transfer Conference*, AIChe Symposium Series No. 225, Vol. 79, pp. 130~139.

Marto, P. J. and Lepere, V. J., 1982, "Pool Boliling Heat Transfer from Enhanced Surfaces to Dielectric Fluids," *J. Heat Transfer*, Vol. 104, pp. 292~299.

Mudawar, I. and Maddox, D. E., 1990, "Enhancement of Critical Heat Flux from High Power Microelectronic Heat Sources in a Flow Channel," *J. Electronic Packaging*, Vol. 112, pp. 241~248.

Nakayama, W., Daikoku, T. and Nakajima, T., 1982, "Effects of Pore Diameters and System Pressure on Saturated Pool Nuclcate-Boiling Heat Transfer from Porous Surfaces," *J. Heat Transfer*, Vol. 104, pp. 286~291.

Nakayama, W., Nakajima, T. and Hirasawa, S., 1984, "Heat Sink Studs Having Enhanced Boiling for Cooling of Microelectronic Components," ASME Paper No. 84-WA/HT-89.

Simon, R. E., 1983, "Thermal Management of Electronic Packages," *Solid State Technology*, pp. 131~137.

Simon, R. E., 1987, "Direct Liquid Immersion Cooling, Past Present and Future," *IBM Technical Report*, No. TR 00. 3465, Poughkeepise, N. Y.

Sturgis, J. C. and Mudawar, I., 1999, "Assessment of CHF Enhancement Mechanisms in a Curved, Rectangular Channel Subjected to Concave Heating," *J. Heat Transfer*, Vol. 121, pp. 394~404.

You, S. M., Bar-Cohen, A. and Simon, T. W., 1990, "Boiling Incipience and Nucleate Boiling Heat Transfer of Highly Wetting Dielectric Fluids from Electric Materials," *IEEE CHMT Trans.*, Vol. 13, pp. 1032~1039.

You, S. M., Simon, T. W. and Bar-Cohen, A., 1990, "Experiment on Nucleate Boiling Heat Transfer With a Highly-Wetting Dielectric Fluid : Effects of Pressure, Subcooling and Dissolved Gas Contents," *Heat Transfer*, Vol. 2, pp. 337~342, Hemisphere Publishing Corp.